

Urban morphology and dynamics with local climate zones in Cuiabá-MT

Diana Carolina Jesus de Paula

PhD, UNIVAG, Brazil.
diana.paula@univag.edu.br

Flávia Maria de Moura Santos

PhD, UFMT, Brazil.
flavia_mms@hotmail.com

Natallia Sanches e Souza

PhD, UNIVAG, Brazil.
natallia@univag.edu.br

Fernanda Miguel Franco

PhD, IFMT, Brazil.
fermigfran@gmail.com

Fabio Friol Guedes de Paiva

PhD, UNIVAG, Brazil.
fabio.paiva@univag.edu.br

Received: May 6, 2024
Accepted: July 31, 2024
Online Published: August 28, 2024

ABSTRACT

It is known that it will be in urban areas that extreme events such as heat waves will occur more intensely as a consequence of climate change, resulting in heat islands. Such events will be more challenging in developing countries with a tropical climate. Urban heat islands at night in the city of Cuiabá-MT have already been identified by several researchers, including increased intensity, therefore the objective of this study was to apply the local climate zones (LCZs) classification system, which aims to classify on a scale local morphology and urban texture, relating it to the thermal field during the years 2011, 2016 and 2019, in order to corroborate the monitoring of the effects of climate change in cities with a tropical climate.

Keywords: local climate zones, urban heat island, urban planning

1 INTRODUCTION

The main cause of global warming is the increased concentration of greenhouse gases in the atmosphere, which absorb and re-emit thermal radiation. This results in more heat being retained in the atmosphere and thus an increase in the global average temperature of the Earth's surface. Causing changes in climate characteristics, such as temperature, humidity, precipitation, wind, and severe weather events over long periods (WMO).

In this context, data available on population growth in urban areas is 70% by 2050 on a global scale, and in Brazil 85.7% (UN, 2020). The physical consequences of climate change on the urban population include extreme events such as heat waves, extreme precipitation, inland and coastal flooding, landslides, increased aridity, water scarcity and air pollution. In this way, climate change challenges us to rethink our urban systems (including transportation and buildings).

Against this backdrop, the period from 2015 to 2019 was the five hottest years on record by the World Meteorological Organization (WMO). The increase over the historical average was 1,3°C, making February 2016 the hottest month in the last 130 years, and July 2016 the hottest July in the last 136 years (NASA, 2016).

In Brazil in 2020, new historical air temperature records were recorded: 44 °C in Cuiabá in 110 years (30/09/2020), 35.5 °C in Curitiba in 110 years (02/10/2020); 41.2 °C in Goiânia in 83 years (07/10/2020) (UN, 2020).

In this sense, strategies are emphasized as responses to current and future climate extremes in the urban context, aimed at mitigation are strategies related to reducing emissions of gases that make up the Greenhouse Effect (GHG), in this perspective Braga (2012), points out that urban planning plays a fundamental role from the urban form, based on land use patterns, which generate displacement demands.

This is reinforced by Bianco et al. (2011), who say that the structure, orientation, and condition of buildings and streets tend to increase the need for cooling and heating of buildings due to the energy balance process between solar radiation that is absorbed and dissipated, according to the properties of the materials in the built environment.

Therefore, research involving climate as a tool for urban planning aimed at adapting to climate change in tropical cities is urgent, given that the demand for cooling is the main strategy (EMMANUEL, 2016). For this reason, urban planning strategies as adaptation measures should cover studies on: Temperature and heat waves, Precipitation, floods and droughts, promoting changes in building codes, land use and occupation laws, restricting the expansion of the urban fabric in vulnerable areas (PBMC, 2016).

In this vein, Stewart & Oke (2012), present a new universal classification method based on Local Climate Zones (LCZs), with the aim of standardizing studies on heat islands. The system comprises the classification of 17 Local Climate Zones, 10 of which are defined by typologies and densification of buildings and 7 types of land cover in addition to surface properties, which exemplify urban morphology and the various uses of land in the processes of transformation and energy production.

A recent study on Cuiabá-MT, considering the last 20 years, shows that the hot-dry period (autumn-winter) has 30% more occurrences than the hot-wet period (spring-summer), with August and September having the highest number of occurrences, These are the months with the highest record of low humidity and fires in the region, i.e. they occurred more frequently during the hot-dry period on 404 days and in the hot-wet period on 289 days, with air temperatures ranging from 37.4°C to 42°C (ROSSO et al, 2023).

In this way, this research aims to relate the LCZ classes that predominated in the City of Cuiabá-MT, a city located in a continental area of Brazil with medium latitude, during the years 2011, 2016 and 2019 with the urban heat island data found in order to corroborate climate change studies in urban centers.

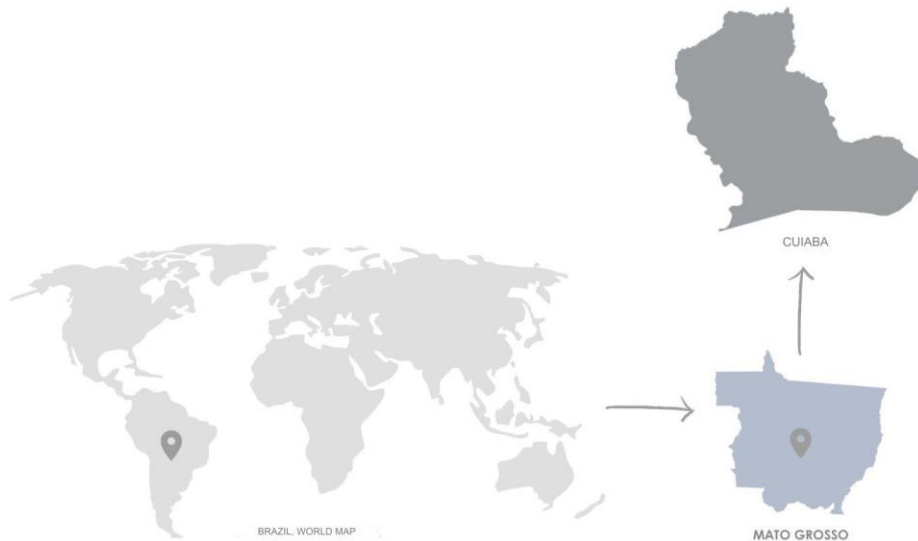
2 MATERIAL AND METHODS

2.1 Study area

Cuiabá-MT is known for its harsh climate, with high temperatures throughout the year. The area of the municipality is 3,538.17km², of which 254.57km² corresponds to the urbanized area occupied by an estimated urban population of 650,877 (IBGE, 2022).

The predominant biome in the municipality (Figure 1) is the Cerrado. The climate profile is tropical continental semi-humid type Aw according to the Köppen classification, with two well-defined seasons, one hot-dry (autumn-winter) and one hot-humid (spring-summer) and daily maximum air temperatures that oscillate between 30°C and 36°C.

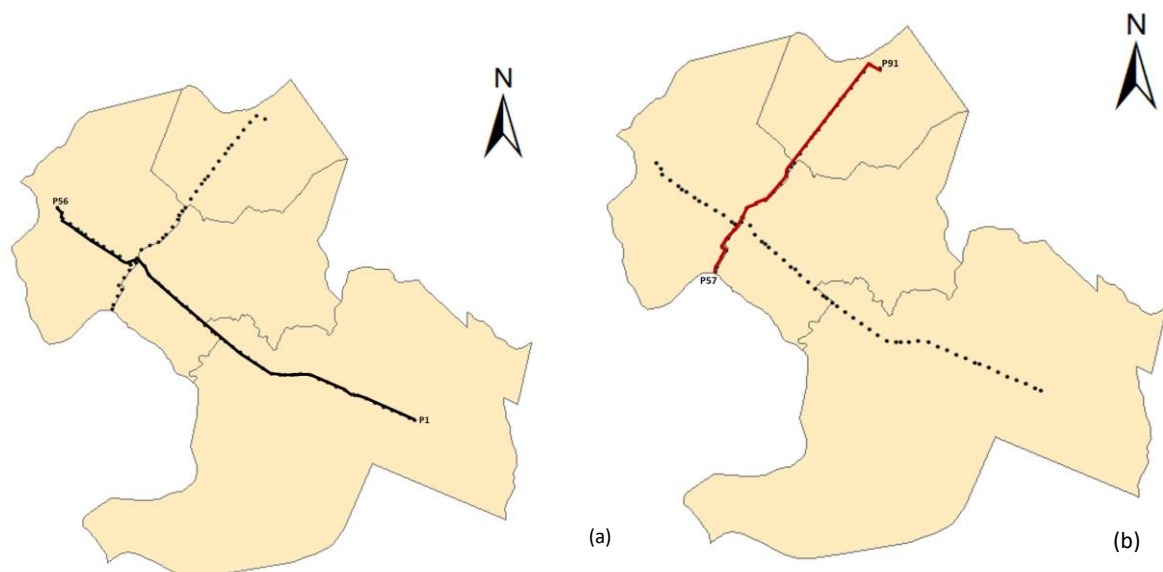
Figure 1 - Location of the municipality of Cuiabá in the state of Mato Grosso - Brazil



The methodology used to collect the climatic variables was a night-time mobile transect with a motor vehicle, a protocol adopted when the route to be taken is very long. The measurements always began at 8 p.m. with vehicle speed varying between 30 and 40 km/h, on days with stable weather conditions, light winds and clear skies (OKE, 2004; AMORIM, 2005; VALIN Jr., 2019) during the years 2011, 2016 and 2019.

Due to the size of the study area, it was decided to divide the data collection into two transects, transect 1 - East/West (Figure 2a) with 56 points covering 19.76km and transect 2 - South/North (Figure 2b) with 35 points covering 11.6km, totaling 91 points.

Figure 2 - Transect 1 (a) and transect 2 (b)



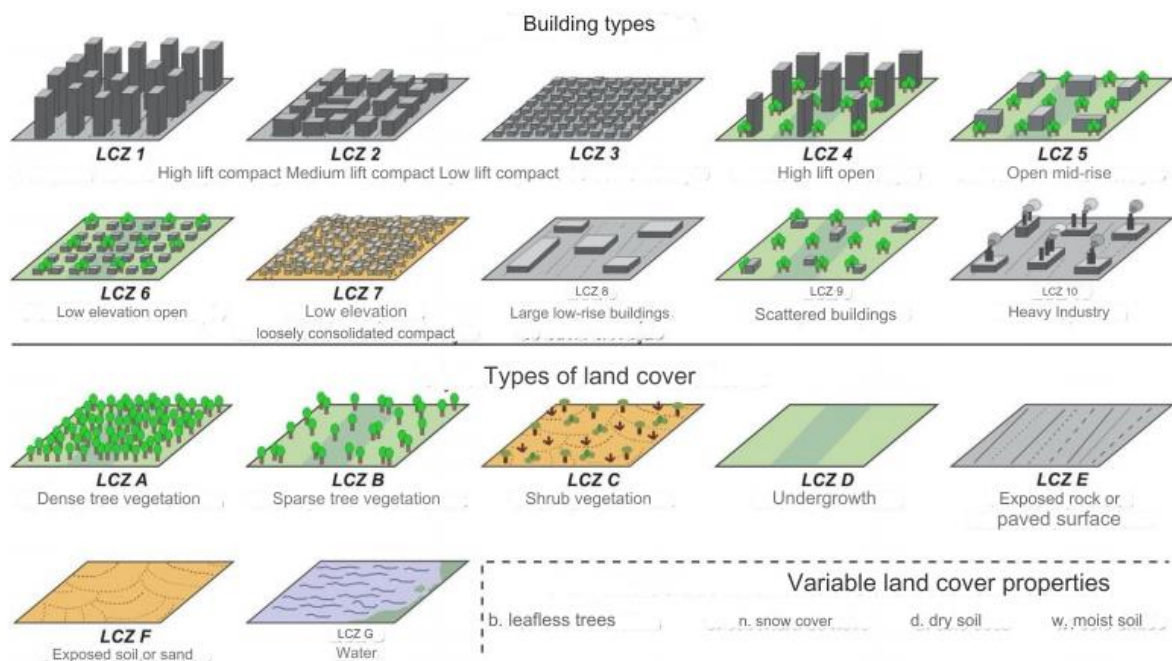
The data collection of climatic variables is part of a research project that began in 2011, continued in 2016 and ended in 2019. A datalogger with GPS, model GK_V02, was used, as well as an air temperature and relative humidity sensor, model DHT22, to measure temperature in the -40 to 125°C range and humidity in the 0 to 100% range. The datalogger was programmed on a Raspberry Pi 3 microcontroller board. The attached GPS module is the GY-GPS6MV2 Ublox model.

The coordinates were transferred to UTM (Universal Transverse Mercator), Zone 21S, for the accuracy of the point measurement locations. All the sensors were protected by a shelter attached to the side of the vehicle, fixed approximately 2.00m off the ground. To validate the data, the values obtained from INMET's automatic station (OMM Code: 86705) for each year on the days measured, located in Cuiabá-MT, were used as reference data.

2.2 Classification based on local climate zones (LCZ)

The LCZ classification used an empirical method of visual analysis of each of the 91 points, starting from a diameter of 400m, to verify the construction typologies that are standardized from LCZ 1 to 10, and for the land cover that is standardized from LCZ A to G (figure 3).

Figure 3 - Building and land cover typologies of Local Climate Zones (LCZ)



Source: Adapted from Stewart and Oke (2012) apud Pinton et al. (2021)

Thematic maps were generated using the supervised classification method, through the MAXVER (maximum similarity) technique, using images from Google Earth software, obtaining the percentages for each class of interest according to Stewart and Oke (2012), i.e. percentage of built, impermeable and permeable cover (Table 1).

Tabela 1 - Valores de propriedades geométricas, cobertura de superfície, propriedades térmicas, radiativas e metabólicas das Zonas Climática Locais (LCZs)

LCZ	SVF (a)	Reason for the urban canyon (b)	Built surface ratio (c)	Impervious area ratio (d)	Permeable area ratio (e)	Height of roughness elements (f)	Terrain roughness class (g)
LCZ 1	0.2-0.4	>2	40-60	40-60	<10	>25	8
LCZ 2	0.3-0.6	0.75-2	40-70	30-50	<20	10-25	6-7
LCZ 3	0.2-0.6	0.75-1.5	40-70	20-50	<30	3-10	6
LCZ 4	0.5-0.7	0.75-1.25	20-40	30-40	30-40	>25	7-8
LCZ 5	0.5-0.8	0.3-0.75	20-40	30-50	20-40	10-25	5-6
LCZ 6	0.6-0.9	0.3-0.75	20-40	20-50	30-60	3-10	5-6
LCZ 7	0.2-0.5	1-2	60-90	<20	<30	2-4	4-5
LCZ 8	>0.7	0.1-0.3	30-50	40-50	<20	3-10	5
LCZ 9	>0.8	0.1-0.25	10-20	<20	60-80	3-10	5-6
LCZ 10	0.6-0.9	0.2-0.5	20-30	20-40	40-50	5-15	5-6
LCZ A	<0.4	>1	<10	<10	>90	3-30	8
LCZ B	0.5-0.8	0.25-0.75	<10	<10	>90	3-15	5-6
LCZ C	0.7-0.9	0.25-1.0	<10	<10	>90	<2	4-5
LCZ D	>0.9	<0.1	<10	<10	>90	<1	3-4
LCZ E	>0.9	<0.1	<10	>90	<10	<0.25	1-2
LCZ F	>0.9	<0.1	<10	<10	>90	<0.25	1-2
LCZ G	>0.9	<0.1	<10	<10	>90	-	1

Source: Adapted from Stewart and Oke (2012)

c- Ratio of the area of the building plan to the total area of the land (%)

d- Ratio of the impervious flat area (paved, rock) in relation to the total flat area of the land (%)

e- Ratio of the permeable flat area (bare soil, vegetation, water) to the total area of the land (%)

Each LCZ will be named individually, ordered by one or more classes, built typologies and land cover typologies, so the code for the subclasses is LCZ Xa, where X is the most predominant class of the LCZ standard set, a is the lowest class (if applicable) of the standard set.

The surface cover properties will be used to verify the influence of urban texture with the microclimatic variables.

2.3 Heat Island Calculation

Stewart and Oke (2012) propose that the heat island be represented by the difference in air temperature between the LCZs, making it possible to analyze the common surfaces and the characteristics of the built typologies and land cover in the comparison of cases, highlighting and facilitating the recognition of urban influences on air temperature.

$$HIU = LCZX - LCZY \quad (\text{equation 01})$$

The magnitude of the observed urban heat island will be related to the LCZs in order to verify which construction typologies have contributed to heating within the study area.

2.4 Data statistics

For data analysis, spreadsheets separated by points were created, relating the data on air temperature, relative humidity, urban heat island, and land cover with the identified LCZs.

The statistical analysis adopted was initially to verify the normality of the data, using the Kolmogorov-Smirnov test, to assess whether the data distribution adheres to Normal, with adherence being rejected with sig.<0.05. After rejecting the hypothesis of normality, the nonparametric Kruskal-Wallis test was adopted to compare the medians of the groups, with significant differences being detected with sig.<0.05, that is, the groups show differences between themselves (TORMAN et. al, 2012).



3 RESULTS AND DISCUSSION

3.1 LCZ Classification

In the classification of each LCZ in points during the years of study, 33 typologies were identified in 2011, 34 in 2016 and 35 in 2019, thus seeking to observe the existence of LCZX that persist in all years. Thus, the LCZX are 2, 4, 8, 9 and A.

The number of points in each of the classes in 2011 were: 47 points as LCZ8, followed by 9 points as LCZ2 and A, 7 points as LCZ9, 5 points as LCZ4, as per Table 2.

Table 2 - LCZ classification during the years 2011, 2016 and 2019

Figures	Description LCZs	Points								
		2011			2016			2019		
	2 – High density of medium height	P43 P70	P44 P46	P67	P43 P47 P67	P44 P63	P45 P66	P40 P63	P44 P67	P47
	2 _A – High density of medium height with dense tree vegetation	P42			P42	P64		P43	P64	
	2 _C – High density of medium height with shrub vegetation							P34		
	2 _D – High density of medium height with low vegetation				P46					
	2 _E – High density of medium height with paved surface	P47	P63	P68				P22	P33 P45 P71	P39 P68
	4 – Medium density at high height	P48	P49 P71	P50 P73	P48	P49 P72	P50	P48	P49 P65 P72	P50
	4 ₂ – Medium density of high height with high density of medium height							P70		
	4 _E – Medium density of high height with paved surface				P51 P70	P68 P71	P69	P51	P69	
	8 – Large low-rise buildings	P21 P69	P34	P62	P34	P85 P86		P20	P36 P38 P85	P37
8 ₂ – Large low-rise buildings with high density of medium-rise buildings	P39			P39	P59 P76	P61 P62	P59	P61 P62		



8 ₃ . Large low-rise buildings with high low-rise density	P31 P60	P36 P61	P40	P25 P40	P31	P36	P60		
8 ₄ . Large low-rise buildings with medium density and high height	P37	P38		P37	P38				
8 ₅ . Large low-rise buildings with medium density of medium height							P29	P76	
8 ₆ . Large low-rise buildings with medium low-rise density							P25	P28 P6	
8 _A . Large, low-rise buildings with dense tree vegetation	P18 P64	P27 P75	P5	P26			P13 P5	P17 P84	P18 P26
8 _B . Large, low-rise buildings with sparse tree vegetation	P10 P28 P84	P11 P6	P20 P82	P14 P28 P6	P15 P29 P9	P18 P5	P10	P82 P9	
8 _C . Large low-rise buildings with shrubby vegetation	P1 P19 P3 P86	P13 P2 P4 P9	P16 P23 P85	P16	P17	P23	P19	P2 P3 P35	
8 _D . Large low-rise buildings with low vegetation	P57	P58		P10 P24	P11 P4	P22	P24		
8 _E . Large low-rise buildings with paved surfaces	P15 P33 P65	P22 P35 P66	P30 P59 P74	P1	P13 P20 P30 P33 P58	P19 P21 P32 P35 P60	P2 P3	P1	P15 P23 P31 P57 P86
8 _F . Large low-rise buildings with exposed soil	P24						P16	P4	



9 - Scattered buildings	P52	P53		P81					
9 ₃ . Sparse buildings with high density and low height							P12		
9 ₄ . Sparse buildings with medium density and high height							P52	P53	
9 ₆ . Sparse buildings with medium density and low height							P11		
9 _A . Sparse buildings with dense tree vegetation	P32	P76	P77	P27	P54		P27	P77 P81	
9 _B . Sparse buildings with sparse tree vegetation	P17			P84					
9 _C . Sparse buildings with shrubby vegetation	P72								
9 _F . Sparse buildings with exposed soil				P74					



A - Dense tree vegetation	P55	P78		P55	P79 P80		P55	P80	
A ₅ . dense tree vegetation with medium density and medium height				P78					
A ₈ . Dense tree vegetation with large, low-rise buildings	P14	P81		P12					
A ₉ . Dense tree vegetation with scattered buildings	P54 P80	P56 P83	P79	P56	P83		P14	P56 P79 P83	P78

In 2016, the number of points in each class is: LCZ8 and 2 have 45 and 10, respectively. An increase was observed in the LCZ4 classes with 9, while the classes with a decrease were LCZA with 7 points and LCZ9 with 5 points.

In 2019, it can be seen that LCZ8 still has the highest number of points, but falling to 40. The classes that showed an increase are LCZ2 with a total of 12 points, LCZ9 with 7 points and LCZ4 with 8 points. However, LCZA has maintained 7 points since 2016.

Therefore, the building typologies that were adopted most frequently are the high density of medium height (LCZ2) and medium density of high height (LCZ4) types in more central areas of the city, wide low-rise buildings (LCZ8), sparsely built (LCZ9) in areas further away from the center, dense tree vegetation (LCZA) present in urban park or permanent preservation areas.

Demonstrating that the city's urban planning has promoted areas with high occupancy rates due to the identification of the LCZ8 class in the largest number of points, in addition to areas with potential for verticalization and densification as a result of the increase in points in LCZ2 and LCZ4. However, as a positive potential, the maintenance of points in areas with dense tree vegetation is observed.

Ferreira & Ugeda Júnior (2020) identified a similar classification using the LCZ system from remote sensing in the urban perimeter of Cuiabá, being in the central region LCZ 2, in more isolated areas and further away from the central region LCZ 4 and LCZ A close to high traffic roads.

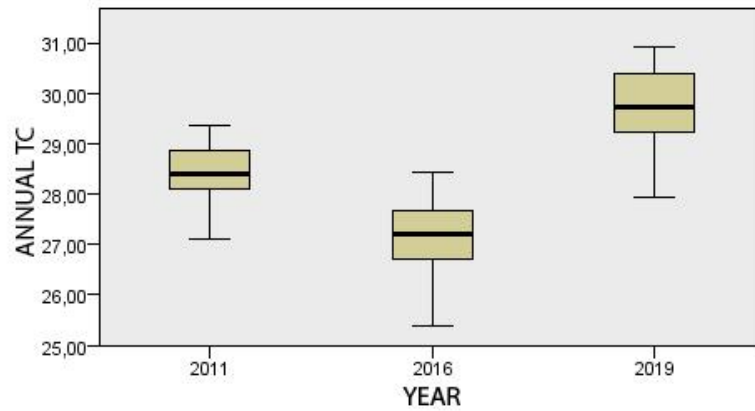
After collecting and processing data on microclimatic variables, average annual air temperature (annual TC) and soil cover values were obtained. Subsequently, the effects of surface properties based on soil cover data and the relationship between LCZs during the study years and HIU were investigated.

3.2. Analysis of air temperature with LCZs and surface properties

The air temperature (ANNUAL TC) in 2011 recorded an average of 28.40°C and in 2016 an average of 27.10°C, with a decrease in the average TC of 1.3°C compared to 2011. However, in 2019 the average was 29.72°C.

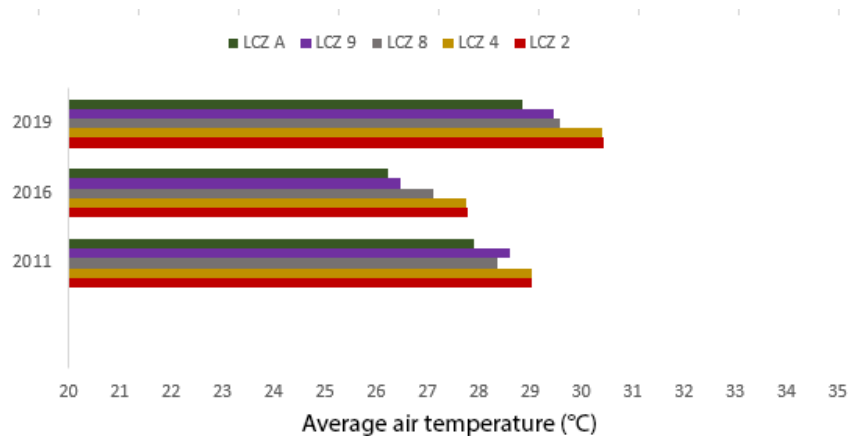
There was an increase in the average TC of 2.62°C compared to 2016, corresponding to an increase of 9.66%. In the period of 8 years, that is, between 2011 and 2019, there was an increase in the average TC of 1.32°C. It is possible to infer that over the course of 8 years the average TC increased by approximately 5%, that is, going from 28.40°C to 29.72°C, as shown in figure 4.

Figure 4 - Air temperature (ANNUAL TC) in 2011, 2016 and 2019



Analyzing the average air temperature of each year with the LCZs (figure 5), it is observed that the highest temperatures are in LCZ2 and 4, which may be related to the urban morphology of the medium density type of medium to high elevation. The lowest records are observed in LCZA, where the thermal field is influenced by the presence of dense tree vegetation due to shading and evapotranspiration.

Figure 5- Relationship between air temperature and LCZs between 2011, 2016 and 2019



Comparisons of the surface properties of each year with the reference values of the identified LCZ classes highlight that LCZs 2, 4 and 8 are those that present the highest densification values according to the references suggested by Stewart & Oke (2012), varying only the height of the building.

LCZs 9 and A are those that present the lowest values for built density, thus in LCZ9 in 2011 and 2019 percentages above the reference values were observed, however a drop was identified in 2016. However, LCZA exceeded the reference limits from 2016 onwards, as can be seen in Table 3.

Table 3 - Comparisons of surface properties for each year with the reference values of the LCZ classes

It is possible to make the following observations, in 8 years, between 2011 and 2019, permeability shows a drop of 4.85%, which may be associated with a 6.13% increase in the built

LCZs	% BUILDS 2011	% BUILDS 2016	% BUILDS 2019	% BUILDS REF.	% PERM. 2011	% PERM. 2016	% PERM. 2019	% PERM. REF.	% WATER PROOF 2011	% WATER PROOF 2016	% WATER PROOF 2019	% WATER PROOF REF.
2	40.90	42.36	46.61	40-70	26.16	22.81	20.32	<20	32.93	34.88	33.07	30-50
4	31.03	36.16	46.41	20-40	35.85	25.07	23.95	30-40	32.92	38.77	29.64	30-40
8	29.30	36.32	34.55	30-50	42.81	34.56	39.42	<20	27.76	29.14	26.03	40-50
9	25.89	14.14	25.24	10.-20	43.55	62.23	50.28	60-80	30.56	23.63	24.47	<20
A	8.75	13.04	10.58	<10	75.41	72.68	73.74	>90	15.85	14.29	15.67	<10

fraction.

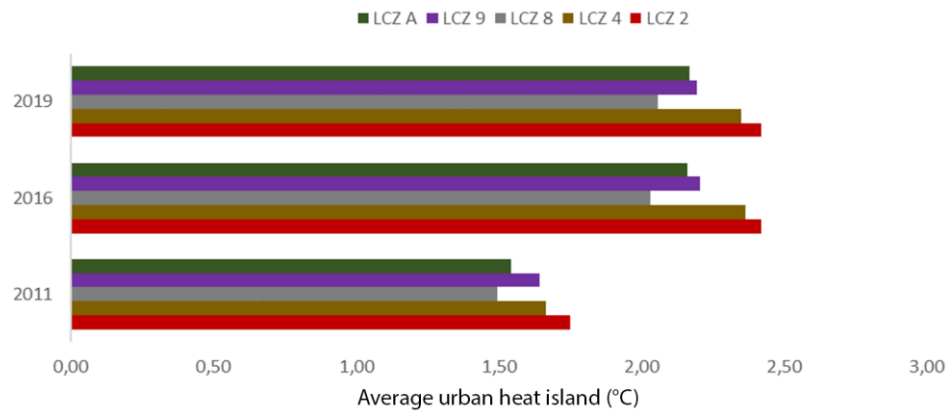
3.3. Analysis of the relationship between the heat island (HIU) and the LCZ classes between the years of study

In 2011, the average heat island ranged from 1.49 to 1.66°C among the LCZ classes, with the high-density, medium-rise typology (LCZ2) expressing the highest average HIU of 1.75°C, followed by the medium-density, high-rise typology (LCZ4) of 1.66°C and sparse buildings (LCZ9) of 1.64°C. However, the typology of large, low-rise buildings (LCZ8) present in most points showed an HIU of 1.49°C, the lowest average observed, but the dense tree vegetation typology (LCZA) showed an average HIU of 1.54°C.

In 2016, the averages varied between 2.03 and 2.42°C, with the highest HIU averages remaining in LCZ2 and LCZ4, at 2.42 and 2.36°C, respectively. This was followed by the sparse building typology (LCZ9) with an HIU of 2.21°C and in LCZA it was 2.16°C, with LCZ8 maintaining the lowest average of 2.03°C.

In 2019, the averages varied between 2.06 and 2.42°C. It can be seen that most classes did not express any change in the HIU average, as in the case of LCZ2 of 2.42°C, LCZ4 of 2.35°C, LCZ 9 of 2.19°C and LCZA of 2.17°. However, there was a slight increase in LCZ8, reaching 2.06°C, as shown in figure 6.

Figure 6 - Relationship between the heat island and the LCZ classes between 2011, 2016 and 2019



In the analysis of the magnitude of the HIU in relation to the LCZs, it is observed that in 5 years, the greatest differences found are in LCZ4 expressing a high of 0.70°C and LCZ2 of 0.67°C with a peak of 2.42°C. It is evident that the majority of the typologies identified in 2016 manifest average HIU values at moderate intensity, that is, greater than 2°C.

In 3 years, between 2016 and 2019, LCZ2 maintained the highest HIU intensity of 2.42°C, as well as LCZ9 and LCZA reaching 2.19°C even when dealing with a typology with an area predominantly of dense tree vegetation. In 8 years, between 2011 and 2019, the largest increase in HIU was in LCZ4 of 0.69°C, followed by LCZ2 of 0.67°C and the smallest was in LCZ9 of 0.55°C.

It is observed that the highest magnitudes of HIU were observed between 2011 and 2016, in the medium-height high-density typology (LCZ2) reaching 2.42°C, followed by the high-height medium-density typologies (LCZ4) expressing 2.36°C. The typologies that expressed the greatest variation were large low-height buildings (LCZ8), sparse buildings (LCZ9) and dense tree vegetation (LCZA), ranging from 1.49 to 2.21°C.

Corroborating the research by Perera & Emmanuel (2018) in Colombo, Sri Lanka, where high and medium density classes tend to have a higher intensity of HIU, however, large low-rise buildings, sparse buildings and ground covers A to F contribute to the variation in the intensity of HIU.

Thus, it is observed that the compact and open arrangement typology with medium-rise buildings (LZC2) tends to have a greater influence on maintaining the intensity of the HIU. On the other hand, the open arrangement typologies with medium-rise buildings (LCZ4) combined with large buildings in sparse arrangements together with the LCZA ground covers tend to influence the variation of the HIU intensity.

Similar results were found in Cuiabá/MT by Ferreira & Ugeda Júnior (2020), when they analyzed the surface temperature and LCZ during the night period, identifying that LCZs with high building density (LCZ2) expressed higher surface temperature.

4. FINAL CONSIDERATIONS

Due to the harsh climate characteristic of the city of Cuiabá/MT, it is essential that the municipality plan to identify strategies for adapting to climate change and mitigating urban heat

islands. In this sense, the use of the methodology based on the LCZ classification to identify thermal variations influenced by urban morphology and texture has proven to be effective.

It is possible to identify that the high-density, medium-rise typology (LZC2) tends to have a greater influence on maintaining the intensity of HIU, however the medium-density, high-rise typologies (LCZ4), wide, low-rise buildings (LCZ8), sparsely built (LCZ 9) tend to influence the variation in the intensity of HIU, thus corroborating research on the heat island effect in tropical climate cities.

From this perspective, urban planning based on climatic aspects for Cuiabá suggests using construction typologies that adopt medium density of medium to low height, with the presence of permeable area. These typologies favor thermal exchanges by convection and the energy balance due to the urban canyon factor, promoting cooling in the nocturnal heat island. Consequently, it is necessary to change the law of land use and occupation through urban indexes and definition of height standards for buildings.

In addition to this, promoting the creation of more areas with LCZA characteristics will create oases by expressing milder temperatures, allowing the mitigation of the heat island effect.

5. BIBLIOGRAPHICAL REFERENCES

- BIANCO, H. et al. The role of urban land in climate change. In: ROSENZWEIG, c. et. alli. **Climate change and cities: First assessment report of the urban climate change research network**. New York: Cambridge University Press, 2011. pp 217-248.
- BRAGA, R. **Mudanças climáticas e planejamento urbano: uma análise do Estatuto da Cidade**. In: Encontro Nacional da Anppas- 4, 2012. Belém-PA-Brasil.
- FERREIRA, H. V. L.; UGEDA JÚNIO, J. C. Variação da temperatura da superfície através de imagens ASTER em Zonas Climáticas Locais da cidade de Cuiabá, Brasil. **Revista Brasileira de Climatologia**. v.26, 2020. p.393-410. ISSN: 2237-8642 (Eletrônica)
- IBGE. Instituto Brasileiro de Geografia e Estatística. Disponível em: <https://cidades.ibge.gov.br/brasil/mt/cuiaba/panorama>. Acessado em 06.06.2022.
- INMET. Instituto Nacional de Meteorologia. Disponível em: <https://bdmep.inmet.gov.br/>
- IPCC – INTERGOVERNMENTAL PANEL ON CLIMATE CHANGE (IPCC). Climate Change 2014: Mitigation of Climate Change. IPCC Working Group III Contribution to AR5. 2014b.
- SANTOS, F. M. M.; NOGUEIRA, M. C. J. A. Análise da influência da ocupação do solo na variação termohigrométrica por meio de transectos noturno em Cuiabá-MT. **Revista Caminhos de Geografia**, v.13, 2012. p.187-194.
- PERERA, N. G. R.; EMMANUL, R. A "Local Climate Zone" based approach to urban planning in Colombo, Sri Lanka. **Urban Climate**, vol. 23, pp. 188-203. <https://doi.org/10.1016/j.uclim.2016.11.006>
- PINTON, L. G.; RIBEIRO, M. C. A.; SUIZU, T. M.; AMORIM, M. C. C. T. Magnitudes do fenômeno da ilha de calor urbana em sacramento (mg): perspectivas de aplicação do sistema das zonas climáticas locais em cidade de pequeno porte. **Revista caminhos da geografia**. v.22, 2021, p.161-179. <http://doi.org/10.14393/RCG227953890>
- STEWART, I. D.; OKE, T. R. Local Climate Zones for Urban Temperature Studies. Bull. **American Meteorological Society**, v. 93, p. 1879–1900, 2012. doi: 10.1175/BAMS-D-11-00019.1
- ONU. Organização das Nações Unidas. Disponível em: <https://nacoesunidas.org/agencia/onuhabitat/>
- OMM. Organização Meteorológica Mundial. Disponível em: <https://news.un.org/pt/tags/omm>
- OKE, T. R. **Initial guidance to obtain representative meteorological observation at urban sites**. Geneva: WMO. 2004.
- OKE, T. R.; MILLS, G.; CHRISTEN, A.; VOOGT, J. A. **Urban climates**. Cambridge: Cambridge University Press, 2017. 542p. ISBN 9781107429536
- PBMC, 2016: Mudanças climáticas e cidades. **Relatório Especial do Painel Brasileiro de Mudanças Climáticas** (Ribeiro, S. K.; SANTOS, A. S. (eds)). PBMC, COPPE – UFRJ. Rio de Janeiro, Brasil. 116p. ISBN: 978-85-285-0344-9.

ROSSO, R. F. ; ENORE, P. T. S. ; SOUZA, N. S ; PAULA, D. C. J. Análise de frequência de eventos extremos de temperatura do ar em centro urbano no cerrado brasileiro. **PERIÓDICO TÉCNICO E CIENTÍFICO CIDADES VERDES**, v. 11, p. 117-186, 2023.

TORMAN, V. B. L.; COSTER, R.; RIBOLDI, J. **Normalidade de variáveis: métodos de verificação e comparação de alguns testes não paramétricos por simulação**. Revista HCPA, 2012. p.227-234.

VALIN Jr., M. O. **Análise de abrigos termo-higrométricos alternativos para transectos móveis**. Cuiabá, 2019. 118f. Tese (Doutorado em Física Ambiental) - Instituto de Física, Programa de Pós-Graduação em Física Ambiental, Universidade Federal de Mato Grosso. Cuiabá, 2019.